



Performance of Cooperative Spectrum Sensing Based on Random Transition of the Primary User in Laplacian Noise

Khushboo Sinha^(✉)  and Y. N. Trivedi 

Nirma University, Ahmedabad 382470, Gujarat, India
{18ftphde24,yogesh.trivedi}@nirmauni.ac.in

Abstract. In this paper, cooperative spectrum sensing (CSS) of dynamic primary user (PU) is considered in Laplacian noise environment. The dynamic PU is characterized by its transitions from ON (present) state to OFF (absent) state and vice-versa. It means, during the entire sensing duration, the PU appears or disappears intermittently. We assume that each cognitive radio (CR) uses conventional test-statistics such as energy detection (ED), absolute value cumulation detection (AVCD) and improved AVCD (i-AVCD). The hard decision from each CR fuses at the fusion center (FC) according to CSS based on OR rule (CSS-OR), CSS-AND rule and CSS-majority rule to make a final decision on the appearance or disappearance of the PU. We further consider dynamic nature of the PU in terms of its arrival rate (θ_A) and departure rate (θ_D). We present performance of the CSS of dynamic PU using receiver operating characteristic (ROC) and detection probability (P_D) versus average signal-to-noise ratio (SNR), denoted by γ , using Monte Carlo simulations. We conclude that the CSS-OR rule based spectrum sensing outperforms CSS-majority rule and CSS-AND rule based spectrum sensing over a wide range of average SNR, i.e., $-10 < \gamma < 10$ dB. We further conclude that CSS-AND rule is unsuitable for enhancing the detection probability of conventional sensing schemes. Furthermore, CSS-majority rule outperforms conventional sensing schemes ED, AVCD and i-AVCD beyond $\gamma = -1$, -5 and -6 dB, respectively.

Keywords: Energy detection · Cooperative spectrum sensing · Fusion center · Dynamic primary user · Laplacian noise · Detection probability

1 Introduction

In the current era of 5G communication, the world has evolved with the massive use of Internet of Things (IoT) devices. Progressive and sound technologies such as cloud computing, big data analytic and wireless communication have led to the widespread use of bandwidth consuming IoT devices [1]. These IoT devices exploit huge bandwidth in the existing limited microwave spectrum and

are extensively used in sectors such as smart manufacturing, smart cities and cyber-physical systems [2]. In the real time scenario, the prevailing microwave spectrum is limited. Although, millimeter wave can relieve spectrum scarcity problem by providing sufficient spectrum, drastic changes in the wireless network are required [3]. Besides the spectrum scarcity problem, the insufficient or under utilization of existing spectrum is a major concern i.e., large segment of the spectrum remains unutilized [4]. The unutilized segment of spectrum is commonly known as spectrum hole [5]. Cognitive radio (CR) is an advanced futuristic and sophisticated technology which uses three major spectrum utilization model, i.e. interweave model, underlay model and overlay model [6]. Amongst which interweave model is the most popular model and sometimes it is also known as opportunistic model [7]. In this model, spectrum holes are periodically or continuously monitored by the unlicensed spectrum user, also known as secondary user (SU), in a way such that licensed user or primary user (PU) suffers minimum interference [6, 7]. The process through which these spectrum holes are sensed to identify the presence of PU is known as spectrum sensing [8].

In CR, there always exists a trade off between the detection probability of PU and the throughput, i.e. with increase in sensing samples, detection probability increases but as a result of no data transmission during sensing period, throughput decreases [9]. The PU traffic which remains steady or varies slowly with time is an ideal assumption for the case of static PU. The assumption of static PU can be well observed in television broadcast and radar systems [10]. On the other hand, dynamic nature of PU is suitable for PU traffic which varies quickly with time as in case of wireless medical networks (medical body area network) and wireless local area network (WLAN) [11]. During the sensing period, the static behaviour of PU is well documented in [12, 13] and dynamic behaviour in [14, 16].

Additive white Gaussian noise (AWGN) has been considered in many spectrum sensing schemes as the noise is assumed to model the thermal noise or Johnson noise in the receiver [17–19]. However, in the current scenario of multi user communications, multiple access interference (MAI) serves as a dominant noise source [20]. In such case, AWGN fails to accurately model the MAI. The MAI is modelled by various noise models such as Laplacian noise model, Gaussian mixture model (GMM) and Middleton Class A model (MCA) [21]. It has been proved that the Laplacian noise model precisely models the MAI in time-hopped ultra-wideband (TH-UWB) wireless communication system under static PU scenario [20, 21]. The CSS, based on majority rule (k_m out of L rule, where $k_m \leq L$), has been considered in Laplacian noise environment under the static PU scenario [22]. In [23], it has been shown that the detection performance of CSS based on Rao detector (CSS-Rao) is superior to the performance based on classical ED (CSS-ED) in non-Gaussian noise, which is modelled by Generalized Gaussian distribution (GGD). In fact, the Laplacian noise and Gaussian distributions are special cases of GGD.

The CSS based on dynamic double threshold energy detection (DDTHED) was proposed in [24] with circularly symmetric Gaussian noise and in the environment of mobile cognitive radio network. It was shown that CSS-DDTHED outperformed CSS-ED.

In this paper, we consider the CSS based on dynamic PU in additive Laplacian noise environment. We assume that there are total L number of CRs and out of which k_m are active CRs. These k_m CRs independently sense the presence of PU by applying test-statistics such as ED [25], absolute value cumulation detection (AVCD) [26] and improved AVCD (i-AVCD) [27]. Then, All CRs send their hard decisions via reporting channel to a central controlling center known as Fusion center (FC). The FC fuses these decisions via different rules such as ‘AND rule’, ‘OR rule’ or ‘majority rule (k_m out of L rule)’. The detection probability and false alarm probability at each active CR are denoted by P_d and P_f , respectively. The detection probability and false alarm probability at the FC are denoted as P_D and P_F , respectively. Further, we assume that the random transitions of the PU, i.e. PU’s random arrival and departure, are modelled by Poisson distribution. Moreover, the random transition time of the PU is modelled by exponential distribution [15].

The rest of the paper is organised as follows. Section 2 presents the system model. Section 3 presents performance analysis of the dynamic PU in detail. Section 4 presents simulation results followed by brief conclusion in Sect. 5.

2 System Model

In the considered dynamic scenario, H_o denotes the hypothesis when PU is present up to a specified sample ψ_o and thereafter PU is absent. In a similar way, H_1 denotes the alternate hypothesis when PU is absent up to a specified sample ψ_1 and thereafter PU is present. Thus, the received signals at each of the L cognitive terminals are expressed as

$$\begin{aligned} H_o : y_k &= \begin{cases} s_k + w_k, & k = 1, \dots, \psi_o \\ w_k, & k = \psi_o + 1, \psi_o + 2, \psi_o + 3 \dots, N \end{cases} \\ H_1 : y_k &= \begin{cases} w_k, & k = 1, \dots, \psi_1 \\ s_k + w_k, & k = \psi_1 + 1, \psi_1 + 2, \psi_1 + 3 \dots, N \end{cases} \end{aligned} \quad (1)$$

where $k = 1, 2, 3 \dots, N$. The N is the aggregate samples present during the sensing period. The s_k is the unknown PU signal and w_k is the Laplacian noise having mean as 0 and variance as $2b_o^2$. The b_o is known as the scale parameter of the Laplacian noise. Average signal-to-noise ratio (SNR) is well expressed as

$$\gamma = \frac{1}{N} \sum_{k=1}^N \frac{s_k^2}{2b_o^2},$$

where ψ_o and ψ_1 indicate the first level transition points of the PU under hypotheses H_o and H_1 respectively. The random transition (departure) of the PU occurs between the samples ψ_o and $\psi_o + 1$ while the random transition (arrival) of the PU occurs between the samples ψ_1 and $\psi_1 + 1$. The probability density function (PDF) of the Laplacian noise is expressed as [22]

$$f_{w_k}(i) = \frac{1}{2b_o} \exp\left(-\frac{|i|}{b_o}\right). \quad (2)$$

Each of the L cognitive terminals then uses ED, AVCD and i-AVCD as test-statistics to decide the presence or absence of PU. Hard decisions from each CR are then sent to FC, where they are fused according to specified CSS fusion rule, i.e., CSS-AND rule, CSS-OR rule and CSS-majority rule. P_F and P_D at the FC can be derived as

$$\begin{aligned} P_F &= \text{Prob}\{H_1|H_o\} = \sum_{i=k_m}^L \binom{L}{i} P_f^i (1 - P_f)^{L-i}, \\ P_D &= \text{Prob}\{H_1|H_1\} = \sum_{i=k_m}^L \binom{L}{i} P_d^i (1 - P_d)^{L-i}, \end{aligned} \quad (3)$$

where P_f and P_d are false alarm probability and detection probability at each L cognitive terminal. k_m denotes the number of active CRs present. $k_m = 1$ represents OR rule, $k_m = L$ represents AND rule and $k_m < L$ represents majority rule.

3 Performance Analysis

In this section, we present two subsections. In the first subsection, we present three different cases of CSS-ED. The first case presents the case static PU as a special case of dynamic PU while the second and third case being the dynamic PU random arrival case and random departure case, respectively. In the second subsection, we presents all the three cases of PU in CSS-i-AVCD. We also discuss AVCD as a special case of i-AVCD. Further, we derive P_D and P_F in each of the considered cases in CSS-ED and CSS-i-AVCD.

3.1 CSS Based on Energy Detection (CSS-ED)

ED is one of the simplest spectrum sensing techniques in the field of cognitive radio. Considering ED as the test-statistic, the likelihood functions under hypothesis H_o and H_1 are expressed as [15]

$$\begin{aligned} f(\mathbf{y}|\mathbf{s}_{co}, H_o) &= \frac{1}{(2b_o)^N} \exp \left\{ - \sum_{k=1}^{\psi_o} \frac{|y_k - s_k|^2}{b_o} - \sum_{k=\psi_o+1}^N \frac{|y_k|^2}{b_o} \right\}, \\ f(\mathbf{y}|\mathbf{s}_{c1}, H_1) &= \frac{1}{(2b_o)^N} \exp \left\{ - \sum_{k=1}^{\psi_1} \frac{|y_k|^2}{b_o} - \sum_{k=\psi_1+1}^N \frac{|y_k - s_k|^2}{b_o} \right\}, \end{aligned} \quad (4)$$

where $\mathbf{y} = [y_1, y_2, y_3 \dots, y_N]$, $\mathbf{s}_{co} = [s_1, s_2, s_3 \dots, s_{\psi_o}]$ and $\mathbf{s}_{c1} = [s_{\psi_1+1}, s_{\psi_1+2}, s_{\psi_1+3} \dots, s_N]$. As s_k is unknown PU signal, it is necessary to omit it from the likelihood function. Maximum likelihood (ML) estimation of s_k is used for this purpose. It results in

$$\frac{f(\mathbf{y}|\hat{\mathbf{s}}_{c1}, H_1)}{f(\mathbf{y}|\hat{\mathbf{s}}_{co}, H_o)} = \frac{\frac{1}{(2b_o)^N} \exp\left\{\sum_{k=1}^{\psi_1} -\frac{|y_k|^2}{b_o}\right\}}{\frac{1}{(2b_o)^N} \exp\left\{\sum_{k=\psi_o+1}^N -\frac{|y_k|^2}{b_o}\right\}} \underset{H_o}{\overset{H_1}{\geq}} \lambda_o, \quad (5)$$

where $\hat{\mathbf{s}}_{co} = [\hat{s}_1, \hat{s}_2, \hat{s}_3, \dots, \hat{s}_{\psi_o}]$ and $\hat{\mathbf{s}}_{c1} = [\hat{s}_{\psi_1+1}, \hat{s}_{\psi_1+2}, \dots, \hat{s}_N]$. \hat{s}_k is the ML estimate of s_k which is calculated manually and found to be y_k , i.e., $\hat{s}_k = y_k$. At this point, ψ_o and ψ_1 are also unknown and random. Simplifying (5), the likelihood ratio test can be expressed as

$$Z_{ED} = \sum_{k=\psi_o+1}^N |y_k|^2 - \sum_{k=1}^{\psi_1} |y_k|^2 \underset{H_o}{\overset{H_1}{\geq}} \lambda'_o, \quad (6)$$

where $\lambda'_o = b_o \cdot \ln(\lambda_o)$ is the threshold and decision statistic is Z_{ED} . It is obtained using Neyman-Pearson (NP) test. The values of ψ_o and ψ_1 are averaged out in (6) over their distributions. The detection probability (P_d) and false alarm probability (P_f) at each CR are expressed as

$$\begin{aligned} P_d &= Pr\left\{Z_{ED} > \lambda'_o | H_1\right\}, \\ P_f &= Pr\left\{Z_{ED} > \lambda'_o | H_o\right\}. \end{aligned} \quad (7)$$

At the FC, hard decisions from each CR using (7) are then forwarded to the FC. The P_D and P_F at the FC are derived from (3). If X denotes random variable signifying PU non-arrival, then its probability mass function (pmf) is expressed as

$$\begin{aligned} f(r; \theta_A T) &= Prob(X = r) \\ &= \frac{\exp\{-\theta_A T\} \cdot \{\theta_A T\}^r}{r!}, \end{aligned} \quad (8)$$

where θ_A denote the PU arrival rate. T is the time interval at which the PU signal is sampled. r denotes the number of occurrence of events (arrivals) within time interval T . Here, we assume $r = 0$. The same case applies when PU randomly departs with θ_D represents the PU departure rate. Hence, the probability with which the PU arrives or departs during sample interval T is given by $1 - \exp\{-\theta_A T\}$ and $1 - \exp\{-\theta_D T\}$, respectively. The probability of the random transition of the PU in the ψ_o^{th} and ψ_1^{th} sample are expressed as [15]

$$\begin{aligned} Prob\{\psi_o\} &= \left\{1 - \exp\{-\theta_D T\}\right\} \cdot \left\{\exp\{-\theta_D T\}\right\}^{\psi_o}, \\ Prob\{\psi_1\} &= \left\{1 - \exp\{-\theta_A T\}\right\} \cdot \left\{\exp\{-\theta_A T\}\right\}^{\psi_1}, \end{aligned} \quad (9)$$

where $Prob\{\psi_o\}$ and $Prob\{\psi_1\}$ are the probability of random departure and random arrival of the PU, respectively. The three cases of PU are discussed in the following sections.

(1) Static PU: Static PU signify a low traffic scenario case when $\psi_o = 0$ and $\psi_1 = 0$. Decision statistic at each L CR which use ED as test-statistic in static scenario is expressed as

$$Z_{ED(s)} = \sum_{k=1}^N |y_k|^2 \underset{H_o}{\overset{H_1}{\gtrless}} \lambda_{ED(s)}, \quad (10)$$

where $\lambda_{ED(s)}$ is the detection threshold of ED based test statistic $Z_{ED(s)}$ obtained by applying NP test. For large values of N , Central limit theorem (CLT) is used to approximate the probability density function (PDF) of $Z_{ED(s)}$ as Gaussian with mean m_s and variance σ_s^2 , i.e.,

$$Z_{ED(s)} \sim N(m_s, \sigma_s^2), \quad (11)$$

where $m_s = 2Nb_o^2$ and $\sigma_s = 2\sqrt{5N}b_o^2$. Using (11), $\lambda_{ED(s)}$ is expressed as

$$\lambda_{ED(s)} = Q^{-1}(P_f)\sigma_s + m_s, \quad (12)$$

where $Q(\cdot)$ represents the Q-function given by $Q(l) = \frac{1}{\sqrt{2\pi}} \int_l^{+\infty} \exp\left(-\frac{t^2}{2}\right) dt$. At the FC, P_F can be obtained using (3).

(2) Random Transition in Dynamic PU (Arrival Case): The case of $\psi_o = 0$ signifies the absence of PU during the complete duration of sensing period. However, it also marks the beginning of transmission of the PU. Here, if we assume ψ_1 follows exponential distribution, then using (6) and (9), decision statistic under this scenario can be obtained as [15,28]

$$\begin{aligned} Z_{ED(a)} &= \sum_{\psi_1=0}^{N-1} \{1 - \exp\{-\theta_A T\}\} \{ \exp\{-\theta_A T\} \}^{\psi_1} \left[\sum_{k=1}^N |y_k|^2 - \sum_{k=1}^{\psi_1} |y_k|^2 \right] \underset{H_o}{\overset{H_1}{\gtrless}} \lambda_{ED(a)} \\ &= \sum_{k=1}^N \left\{ 1 - \exp\{-\theta_A T k\} \right\} |y_k|^2 \underset{H_o}{\overset{H_1}{\gtrless}} \lambda_{ED(a)}, \end{aligned} \quad (13)$$

where $\lambda_{ED(a)}$ is the detection threshold of ED based decision statistic $Z_{ED(a)}$ during PU random arrival. In this case, it can be seen that the arrival time of the PU follows exponential distribution within sensing period. For large values of N , CLT can be applied so that $Z_{ED(a)}$ tends to be Gaussian with mean μ_{A_o} and variance $\sigma_{A_o}^2$. Thus, $\lambda_{ED(a)}$ is expressed as

$$\lambda_{ED(a)} = Q^{-1}(P_f)\sigma_{A_o} + \mu_{A_o}, \quad (14)$$

where μ_{A_o} denotes the mean and $\sigma_{A_o}^2$ denotes the variance of the decision statistic $Z_{ED(a)}$ obtained in (13) under hypothesis H_o . The expression of μ_{A_o} and $\sigma_{A_o}^2$ can be derived and expressed as [28]

$$\begin{aligned}\mu_{A_o} &= \mu_s \left\{ N - \left(\frac{\exp(-\theta_A T) \{1 - \exp(-\theta_A T N)\}}{1 - \exp(-\theta_A T)} \right) \right\}, \\ \sigma_{A_o}^2 &= \sigma_s^2 \left\{ N - \left(\frac{\exp(-2(\theta_A T + 1)) \{1 - \exp(1 - N)\}}{1 - \exp(-1)} + \exp(-2\theta_A T) \right) \right\},\end{aligned}\quad (15)$$

where μ_s and σ_s^2 denotes the mean and variance of the decision statistic $Z_{ED(s)}$ which can be obtained from (11). At the FC, P_F is obtained using (3).

(3) Random Transition in Dynamic PU (Departure Case): The case of $\psi_1 = 0$ signifies the presence of PU during the whole sensing period. However, it also marks the beginning of the last phase of the PU active transmission. Here, if we assume ψ_o follows exponential distribution, then using (6) and (9), decision statistic under this scenario is expressed as

$$\begin{aligned}Z_{ED(d)} &= \sum_{\psi_o=0}^{N-1} \{1 - \exp\{-\theta_D T\}\} \{ \exp\{-\theta_D T\} \}^{\psi_o} \left[\sum_{k=1}^N |y_k|^2 - \sum_{k=1}^{\psi_o} |y_k|^2 \right] \underset{H_o}{\overset{H_1}{\gtrless}} \lambda_{ED(d)} \\ &= \sum_{k=1}^N \left\{ 1 - \exp\{-\theta_D T k\} \right\} |y_k|^2 \underset{H_o}{\overset{H_1}{\gtrless}} \lambda_{ED(d)},\end{aligned}\quad (16)$$

where $\lambda_{ED(d)}$ is the detection threshold of decision statistic $Z_{ED(d)}$ when PU randomly departs. In this case, it can be seen that the departure time of the PU follows exponential distribution within sensing period. For large values of N , by applying CLT, $Z_{ED(d)}$ tends to be Gaussian with mean μ_{D_o} and variance $\sigma_{D_o}^2$. Thus, $\lambda_{ED(d)}$ is expressed as

$$\lambda_{ED(d)} = Q^{-1}(P_f) \sigma_{D_o} + \mu_{D_o}, \quad (17)$$

where μ_{D_o} denote the mean and $\sigma_{D_o}^2$ denote the variance of the decision statistic $Z_{ED(d)}$ obtained in (16) under hypothesis H_o . The expression of μ_{D_o} and $\sigma_{D_o}^2$ can be derived and expressed as [28]

$$\begin{aligned}\mu_{D_o} &= \mu_s \left\{ N - \left(\frac{\exp(-\theta_D T) \{1 - \exp(-\theta_D T N)\}}{1 - \exp(-\theta_D T)} \right) \right\}, \\ \sigma_{D_o}^2 &= \sigma_s^2 \left\{ N - \left(\frac{\exp(-2(\theta_D T + 1)) \{1 - \exp(1 - N)\}}{1 - \exp(-1)} + \exp(-2\theta_D T) \right) \right\},\end{aligned}\quad (18)$$

where μ_s and σ_s^2 are the mean and variance of the decision statistic $Z_{ED(s)}$ which is from (11). At the FC, P_F is obtained using (3).

3.2 CSS Based on i-AVCD (CSS-i-AVCD)

In the scenario of Laplacian noise, AVCD and i-AVCD are the two actively used test-statistics. In i-AVCD, received samples at the cognitive terminal are raised to a positive exponent P in the range $0 < P \leq 2$. Being a special case of i-AVCD at $P = 1$, AVCD test-statistic's corresponding parameters can be obtained by substituting the value of $P = 1$ in the expressions obtained for i-AVCD. Considering i-AVCD as the test-statistic, the likelihood functions under hypothesis H_o and H_1 are expressed as

$$\begin{aligned} f(\mathbf{y}|\mathbf{s}_{co}, H_o) &= \frac{1}{(2b_o)^N} \exp \left\{ - \sum_{k=1}^{\psi_o} \frac{|y_k - s_k|^P}{b_o} - \sum_{k=\psi_o+1}^N \frac{|y_k|^P}{b_o} \right\}, \\ f(\mathbf{y}|\mathbf{s}_{c1}, H_1) &= \frac{1}{(2b_o)^N} \exp \left\{ - \sum_{k=1}^{\psi_1} \frac{|y_k|^P}{b_o} - \sum_{k=\psi_1+1}^N \frac{|y_k - s_k|^P}{b_o} \right\}, \end{aligned} \quad (19)$$

As s_k is unknown PU signal, it is necessary to omit it from the likelihood function. Maximum likelihood (ML) estimation of s_k is used for this purpose. It results in

$$\frac{f(\mathbf{y}|\hat{\mathbf{s}}_{c1}, H_1)}{f(\mathbf{y}|\hat{\mathbf{s}}_{co}, H_o)} = \frac{\frac{1}{(2b_o)^N} \exp \left\{ \sum_{k=1}^{\psi_1} -\frac{|y_k|^P}{b_o} \right\}}{\frac{1}{(2b_o)^N} \exp \left\{ \sum_{k=\psi_o+1}^N -\frac{|y_k|^P}{b_o} \right\}} \underset{H_o}{\overset{H_1}{\geq}} \lambda_m, \quad (20)$$

where $\hat{\mathbf{s}}_{co} = [\hat{s}_1, \hat{s}_2, \hat{s}_3, \dots, \hat{s}_{\psi_o}]$ and $\hat{\mathbf{s}}_{c1} = [\hat{s}_{\psi_1+1}, \hat{s}_{\psi_1+2}, \dots, \hat{s}_N]$. \hat{s}_k is the ML estimate of s_k which is calculated manually and found to be y_k , i.e., $\hat{s}_k = y_k$. Simplifying (20), the expression becomes

$$Z_{i-AVCD} = \sum_{k=\psi_o+1}^N |y_k|^P - \sum_{k=1}^{\psi_1} |y_k|^P \underset{H_o}{\overset{H_1}{\geq}} \lambda'_m, \quad (21)$$

where λ'_m is the detection threshold of decision statistic Z_{i-AVCD} which is equal to $b_o \cdot \ln(\lambda_m)$. It is obtained using Neyman-Pearson (NP) test. Detection Probability (P_d) and false alarm probability (P_f) at each CR are expressed as

$$\begin{aligned} P_d &= Pr \left\{ Z_{i-AVCD} > \lambda'_m | H_1 \right\}, \\ P_f &= Pr \left\{ Z_{i-AVCD} > \lambda'_m | H_o \right\}. \end{aligned} \quad (22)$$

At the FC, hard decisions from each CR using (22) are then forwarded to the FC. The P_D and P_F at the FC are derived from (3). The probability of the random transition of the PU in the ψ_o^{th} and ψ_1^{th} sample can be derived from (9).

(1) Static PU: Static PU signify a low traffic scenario case when $\psi_o = 0$ and $\psi_1 = 0$. Decision statistic at each L CR which use i-AVCD as test-statistic in static scenario is expressed as

$$Z_{i-AVCD(s)} = \sum_{k=1}^N |y_k|^P \underset{H_o}{\overset{H_1}{\gtrless}} \lambda_{i-AVCD(s)}, \quad (23)$$

where $\lambda_{i-AVCD(s)}$ is the detection threshold of i-AVCD based test statistic $Z_{i-AVCD(s)}$ obtained by applying NP test. For large values of N , Central limit theorem (CLT) is used to approximate the probability density function (PDF) of $Z_{i-AVCD(s)}$ as Gaussian with mean m_s and variance σ_s^2 , i.e.,

$$Z_{i-AVCD(s)} \sim N(\mu_o, \sigma_o^2), \quad (24)$$

where μ_o and σ_o^2 can be expressed as

$$\begin{aligned} \mu_o &= b_o^P \Gamma(P+1) \\ \sigma_o^2 &= b_o^{2P} (\Gamma(2P+1) - \Gamma^2(P+1)), \end{aligned} \quad (25)$$

where $\Gamma(v) = \int_0^{+\infty} e^{-t} t^{v-1} dt$ [29]. Using (24), $\lambda_{i-AVCD(s)}$ is expressed as

$$\lambda_{i-AVCD(s)} = Q^{-1}(P_f) \sigma_o + \mu_o, \quad (26)$$

where $Q(\cdot)$ represents the Q-function given by $Q(l) = \frac{1}{\sqrt{2\pi}} \int_l^{+\infty} \exp\left(-\frac{t^2}{2}\right) dt$. At the FC, P_F can be obtained using (3).

(2) Random Transition in Dynamic PU (Arrival Case): The case of $\psi_o = 0$ signifies the absence of PU during the complete duration of sensing period. However, it also marks the beginning of transmission of the PU. Using (9) and (21), decision statistic under this scenario can be obtained as

$$\begin{aligned} Z_{i-AVCD(a)} &= \sum_{\psi_1=0}^{N-1} \{1 - \exp\{-\theta_A T\}\} \{ \exp\{-\theta_A T\} \}^{\psi_1} \left[\sum_{k=1}^N |y_k|^P - \sum_{k=1}^{\psi_1} |y_k|^P \right] \\ &= \sum_{k=1}^N \left\{ 1 - \exp\{-\theta_A T k\} \right\} |y_k|^P \underset{H_o}{\overset{H_1}{\gtrless}} \lambda_{i-AVCD(a)}, \end{aligned} \quad (27)$$

where $\lambda_{i-AVCD(a)}$ is the detection threshold of i-AVCD based decision statistic $Z_{i-AVCD(a)}$ during PU random arrival. For large values of N , CLT can be applied so that $Z_{i-AVCD(a)}$ tends to be Gaussian with mean μ_{A_o} and variance $\sigma_{A_o}^2$. Thus, $\lambda_{i-AVCD(a)}$ is expressed as

$$\lambda_{i-AVCD(a)} = Q^{-1}(P_f) \sigma_{A_o} + \mu_{A_o}, \quad (28)$$

where μ_{A_o} denotes the mean and $\sigma_{A_o}^2$ denotes the variance of the decision statistic $Z_{i-AVCD(a)}$ obtained in (27) under hypothesis H_o . The expression of μ_{A_o} and $\sigma_{A_o}^2$ can be derived and expressed as

$$\begin{aligned} \mu_{A_o} &= \mu_o \left\{ N - \left(\frac{\exp(-\theta_A T) \{1 - \exp(-\theta_A T N)\}}{1 - \exp(-\theta_A T)} \right) \right\}, \\ \sigma_{A_o}^2 &= \sigma_o^2 \left\{ N - \left(\frac{\exp(-2(\theta_A T + 1)) \{1 - \exp(1 - N)\}}{1 - \exp(-1)} + \exp(-2\theta_A T) \right) \right\}, \end{aligned} \tag{29}$$

where μ_o and σ_o^2 denotes the mean and variance of the decision statistic $Z_{i-AVCD(s)}$ which can be obtained from (24). At the FC, P_F is obtained using (3).

(3) Random Transition in Dynamic PU (Departure Case): The case of $\psi_1 = 0$ signifies the presence of PU during the whole sensing period. However, it also marks the beginning of the last phase of the PU active transmission. Using (9) and (21), decision statistic under this scenario is expressed as

$$\begin{aligned} Z_{i-AVCD(d)} &= \sum_{\psi_o=0}^{N-1} \{1 - \exp\{-\theta_D T\}\} \{ \exp\{-\theta_D T\} \}^{\psi_o} \left[\sum_{k=1}^N |y_k|^P - \sum_{k=1}^{\psi_o} |y_k|^P \right] \\ &= \sum_{k=1}^N \left\{ 1 - \exp\{-\theta_D T k\} \right\} |y_k|^P \underset{H_o}{\overset{H_1}{\gtrless}} \lambda_{i-AVCD(d)}, \end{aligned} \tag{30}$$

where $\lambda_{i-AVCD(d)}$ is the detection threshold of decision statistic $Z_{i-AVCD(d)}$ when PU randomly departs. For large values of N , by applying CLT, $Z_{i-AVCD(d)}$ tends to be Gaussian with mean μ_{D_o} and variance $\sigma_{D_o}^2$. Thus, $\lambda_{i-AVCD(d)}$ is expressed as

$$\lambda_{i-AVCD(d)} = Q^{-1}(P_f) \sigma_{D_o} + \mu_{D_o}, \tag{31}$$

where μ_{D_o} denote the mean and $\sigma_{D_o}^2$ denote the variance of the decision statistic $Z_{i-AVCD(d)}$ obtained in (30) under hypothesis H_o . The expression of μ_{D_o} and $\sigma_{D_o}^2$ can be derived and expressed as

$$\begin{aligned} \mu_{D_o} &= \mu_o \left\{ N - \left(\frac{\exp(-\theta_D T) \{1 - \exp(-\theta_D T N)\}}{1 - \exp(-\theta_D T)} \right) \right\}, \\ \sigma_{D_o}^2 &= \sigma_o^2 \left\{ N - \left(\frac{\exp(-2(\theta_D T + 1)) \{1 - \exp(1 - N)\}}{1 - \exp(-1)} + \exp(-2\theta_D T) \right) \right\}, \end{aligned} \tag{32}$$

where μ_o and σ_o^2 are the mean and variance of the decision statistic $Z_{i-AVCD(s)}$ which is obtained from (24). At the FC, P_F is obtained using (3).

4 Results

In this section, performance of the CSS in dynamic PU environment with additive Laplacian noise is presented in terms of receiver operating characteristic (ROC) and P_D vs. γ using Monte Carlo simulations. The values of ψ_o and ψ_1 are taken to be 10 and 15 respectively. For static PU environment, $\psi_o = 0$ and $\psi_1 = 0$. Similarly, for random transitions of the PU, i.e., in dynamic environment, both are less than N . We have used constant value of $P = 0.8$ throughout our simulation results as it is known that the detection performance of i-AVCD improves with decrease in the value of P and vice-versa in the presence of Laplacian noise. Further, the value of N is also assumed to be constant at $N = 50$ as detection performance improves with increase in the value of N and vice-versa. The value of b_o is assumed to be 1 throughout our simulation result.

Figure 1 shows the ROC comparison of conventional i-AVCD with CSS-OR in case when there is random transition of the PU. The values of $\theta_A T$, $\theta_D T$ are assumed to be 10 and 0.1. N is assumed to be 50 and $\gamma = -2$ dB. It is observed that the performance in the dynamic scenario outperforms the performance in the static scenario for $\theta_A T = 10$ while the same is not true for $\theta_A T = 0.1$. We have further observed that the performance of CSS-OR based on test-statistic i-AVCD is better than the performance achieved with conventional i-AVCD.

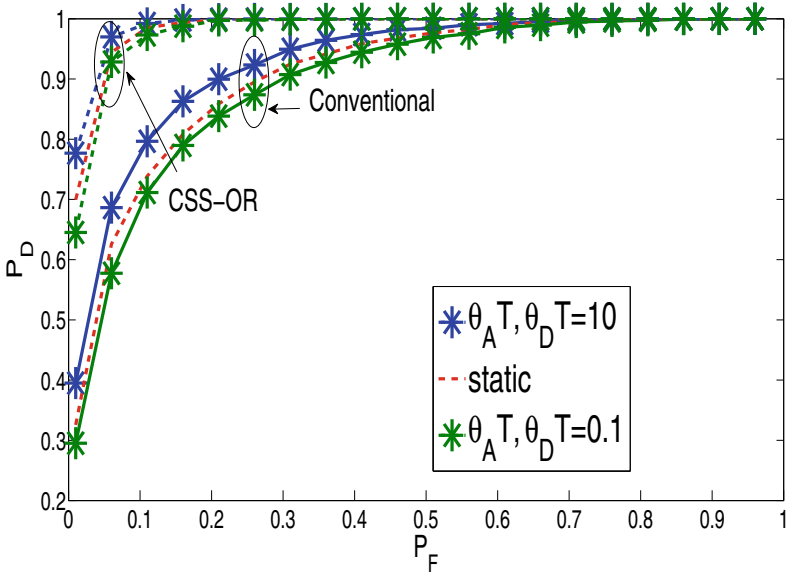


Fig. 1. Comparison of ROC plots for i-AVCD based on conventional scheme and CSS-OR fusion scheme with $N = 50$, $\gamma = -2$ dB, $\theta_A T = 10$ and $\theta_D T = 0.1$.

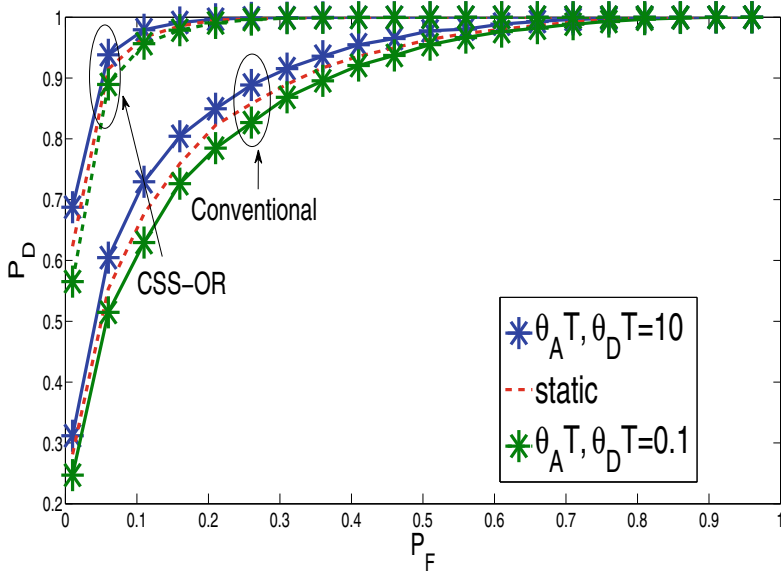


Fig. 2. Comparison of ROC plots for AVCD based on conventional scheme and CSS-OR fusion scheme with $N = 50$, $\gamma = -2$ dB, $\theta_{AT} = 10$ and $\theta_{DT} = 0.1$

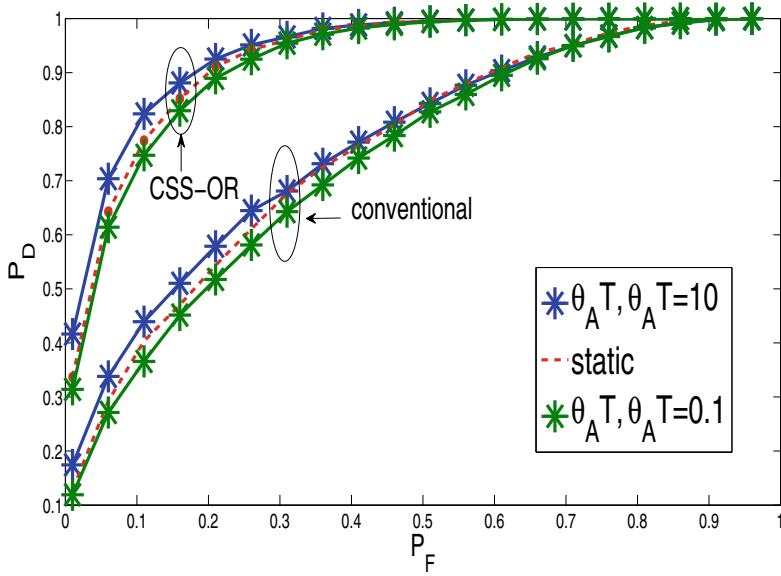


Fig. 3. Comparison of ROC plots for ED based on conventional scheme and CSS-OR scheme with $N = 50$, $\gamma = -2$ dB, $\theta_{AT} = 10$ and $\theta_{DT} = 0.1$

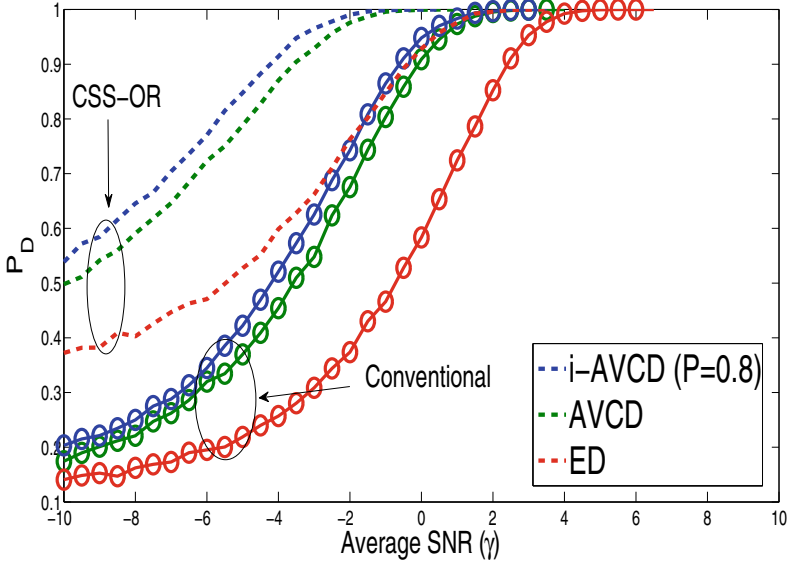


Fig. 4. P_D vs γ comparison of conventional and CSS-OR based test-statistic at $N = 50$, $P = 0.8$ and $P_F = 0.1$ when PU randomly arrives or departs.

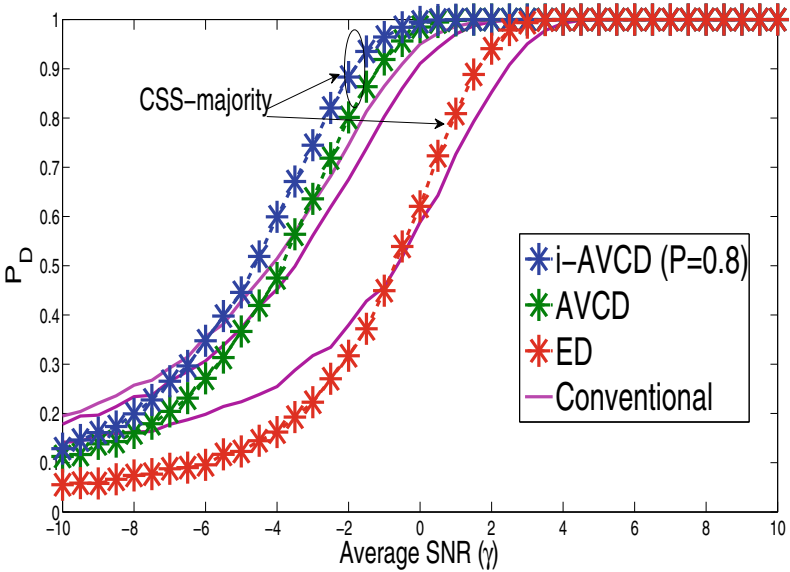


Fig. 5. P_D vs γ comparison of conventional and CSS-majority based test-statistic at $N = 50$, $P = 0.8$, $k_m = 2$, $L = 3$ and $P_F = 0.1$ when PU randomly arrives or departs.

Figure 2 shows the ROC comparison of conventional AVCD with CSS-OR based AVCD. The values of θ_{AT} , θ_{DT} are assumed to be 10 and 0.1. N is assumed to be 50 and $\gamma = -2$ dB. It can be seen that the detection performance in the dynamic PU case outperforms the case of static PU for $\theta_{AT} = 10$. We have further observed that the performance of AVCD based on CSS-OR improves over conventional AVCD.

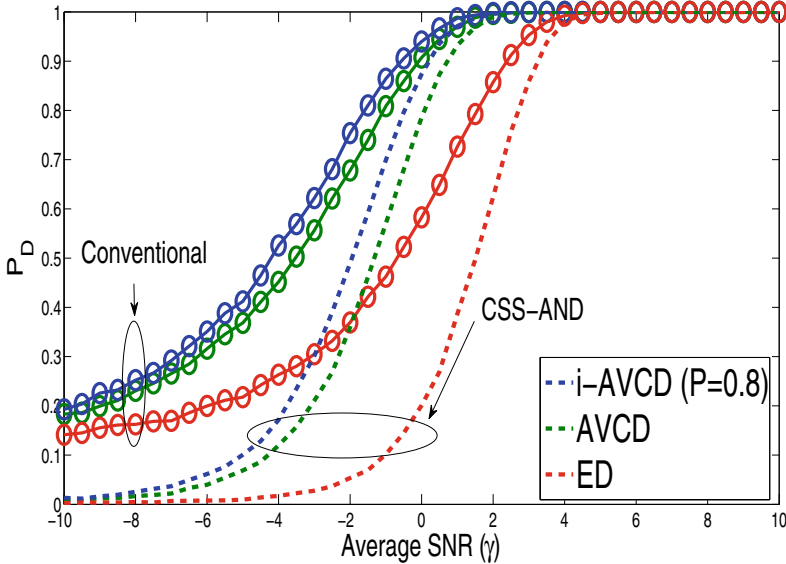


Fig. 6. P_D vs γ comparison of conventional and CSS-AND based test-statistic at $N = 50$, $P = 0.8$ and $P_F = 0.1$ when PU randomly arrives or departs.

Similarly, Fig. 3 shows the ROC comparison of conventional ED with CSS-OR based ED. The values of θ_{AT} , θ_{DT} are assumed to be 10 and 0.1. N is assumed to be 50 and $\gamma = -2$ dB. It is observed that the performance in the dynamic scenario is better than the performance in the case of static PU. We have further observed that the performance of CSS-OR based on ED improves over the performance achieved with conventional ED.

In Fig. 4, we represent detection performance of CSS-OR based on i-AVCD, AVCD and ED based test-statistic for θ_{AT} , $\theta_{DT} = 1$ with $P = 0.8$, $N = 50$ and γ ranges from -10 to 10 dB with an interval of 0.5 dB. We have observed that the detection probability improves in case of CSS-OR scheme over that of conventional scheme.

Figure 5 represents detection performance of CSS-majority ($k_m = 2$ out of $L = 3$ CRs) based on i-AVCD, AVCD and ED test-statistic for θ_{AT} , $\theta_{DT} = 1$ with $P = 0.8$, $N = 50$ and γ ranges from -10 to 10 dB with an interval of 0.5 dB. Here, we have observed that for a specified low range of SNR, conventional scheme perform better while for a specified high range of SNR, CSS-majority

based test-statistic perform better. CSS-majority scheme outperform conventional ED, AVCD and i-AVCD beyond -1 , -5 , -6 dB, respectively.

In Fig. 6, we represent detection performance of CSS-AND based on i-AVCD, AVCD and ED based test-statistic for θ_{AT} , $\theta_{DT} = 1$ with $P = 0.8$, $N = 50$ and γ ranges from -10 to 10 dB with an interval of 0.5 dB. Here, we have observed that for the considered wide range of SNR, conventional scheme performs better than CSS-AND scheme.

5 Conclusion

In this paper, we considered the CSS scheme over the conventional sensing schemes such as ED, AVCD and i-AVCD in the additive Laplacian noise environment. Further, we considered the dynamic nature of primary user in terms of θ_{AT} and/or θ_{DT} assuming its random transition within the sensing interval. We presented the detection performance of the considered spectrum sensing schemes using simulations in terms of receiver operating characteristics and detection probability versus average SNR. We conclude that CSS-OR scheme outperforms conventional sensing schemes over a wide SNR range of $-10 < \gamma < 10$ dB. It is because, in CSS-OR rule, there exists at least one CR which have local decision based on hypothesis H_1 . Hence, CSS-OR rule is much reserved to let CRs access the licensed band. Also, interference caused to the PU is minimized drastically. Conventional scheme outperforms CSS-AND scheme over the considered SNR range. Hence, we conclude that CSS-AND scheme is unsuitable for enhancing the detection probability of conventional schemes unlike that in the case of Gaussian noise. Further, we also conclude that CSS-majority scheme outperforms the conventional schemes beyond specified values of SNR which is -1 , -5 , -6 dB, respectively, for ED, AVCD and i-AVCD.

References

1. Li, F., Lam, K., Li, X., Sheng, Z., Hua, J., Wang, L.: Advances and emerging challenges in cognitive internet-of-things. *IEEE Trans. Indus. Inform.* **16**(8), 5489–5496 (2020). <https://doi.org/10.1109/TII.2019.2953246>
2. Lin, H., Hu, J., Ma, J., Xu, L., Yu, Z.: A secure collaborative spectrum sensing strategy in cyber-physical systems. *IEEE Access* **5**, 27679–27690 (2017). <https://doi.org/10.1109/ACCESS.2017.2767701>
3. Rappaport, T.S., et al.: Wireless communications and applications above 100 GHz: opportunities and challenges for 6G and beyond. *IEEE Access* **7**, 78729–78757 (2019). <https://doi.org/10.1109/ACCESS.2019.2921522>
4. Karimzadeh, M., Rabiei, A.M., Olfat, A.: Soft-limited polarity-coincidence-array spectrum sensing in the presence of non-gaussian noise. *IEEE Trans. Veh. Technol.* **66**(2), 1418–1427 (2017). <https://doi.org/10.1109/TVT.2016.2570139>
5. Choi, K.W., Hossain, E.: Opportunistic access to spectrum holes between packet bursts: a learning-based approach. *IEEE Trans. Wirel. Commun.* **10**(8), 2497–2509 (2011). <https://doi.org/10.1109/TWC.2011.060711.100154>

6. Liang, Y., Chen, K., Li, G.Y., Mahonen, P.: Cognitive radio networking and communications: an overview. *IEEE Trans. Veh. Technol.* **60**(7), 3386–3407 (2011). <https://doi.org/10.1109/TVT.2011.2158673>
7. Wang, W., Zhang, H.: Slotted secondary transmission with adaptive modulation and coding under interweave cognitive radio. *IEEE Trans. Veh. Technol.* **68**(5), 4800–4809 (2019). <https://doi.org/10.1109/TVT.2019.2904285>
8. Ali, A., Hamouda, W.: Advances on spectrum sensing for cognitive radio networks: theory and applications. *IEEE Commun. Surv. Tutor.* **19**(2), 1277–1304 (2017). <https://doi.org/10.1109/COMST.2016.2631080>
9. Liang, Y., Zeng, Y., Peh, E.C.Y., Hoang, A.T.: Sensing-throughput tradeoff for cognitive radio networks. *IEEE Trans. Wirel. Commun.* **7**(4), 1326–1337 (2008). <https://doi.org/10.1109/TWC.2008.060869>
10. Tang, L., Chen, Y., Hines, E.L., Alouini, M.: Performance analysis of spectrum sensing with multiple status changes in primary user. *Traffic* **16**(6), 874–877 (2012). <https://doi.org/10.1109/LCOMM.2012.041112.120507>
11. Zandi, M., Dong, M., Grami, A.: Distributed stochastic learning and adaptation to primary traffic for dynamic spectrum access. *IEEE Trans. Wirel. Commun.* **15**(3), 1675–1688 (2016). <https://doi.org/10.1109/TWC.2015.2495154>
12. Liu, M., Zhao, N., Li, J., Leung, V.C.M.: Spectrum sensing based on maximum generalized correntropy under symmetric alpha stable noise. *IEEE Trans. Veh. Technol.* **68**(10), 10262–10266 (2019). <https://doi.org/10.1109/TVT.2019.2931949>
13. Zou, Y., Yao, Y., Zheng, B.: Outage probability analysis of cognitive transmissions: Impact of spectrum sensing overhead. *IEEE Trans. Wirel. Commun.* **9**(8), 2676–2688 (2010). <https://doi.org/10.1109/TWC.2010.061710.100108>
14. Pradhan, H., Kalamkar, S.S., Banerjee, A.: Sensing-throughput tradeoff in cognitive radio with random arrivals and departures of multiple primary users. *IEEE Commun. Lett.* **19**(3), 415–418 (2015). <https://doi.org/10.1109/LCOMM.2015.2393305>
15. Beaulieu, N.C., Chen, Y.: Improved energy detectors for cognitive radios with randomly arriving or departing primary users. *IEEE Signal Process. Lett.* **17**(10), 867–870 (2010). <https://doi.org/10.1109/LSP.2010.2064768>
16. Chang, K., Senadji, B.: Spectrum sensing optimisation for dynamic primary user signal. *IEEE Trans. Commun.* **60**(12), 3632–3640 (2012). <https://doi.org/10.1109/TCOMM.2012.091712.110856>
17. Unnikrishnan, J., Veeravalli, V.V.: Algorithms for dynamic spectrum access with learning for cognitive radio. *IEEE Trans. Signal Process.* **58**(2), 750–760 (2010). <https://doi.org/10.1109/TSP.2009.202>
18. MacDonald, S., Popescu, D.C., Popescu, O.: Analyzing the performance of spectrum sensing in cognitive radio systems with dynamic PU activity. *IEEE Commun. Lett.* **21**(9), 2037–2040 (2017). <https://doi.org/10.1109/LCOMM.2017.2705126>
19. Yilmaz, Y., Guo, Z., Wang, X.: Sequential joint spectrum sensing and channel estimation for dynamic spectrum access. *IEEE J. Sel. Areas Commun.* **32**(11), 2000–2012 (2014). <https://doi.org/10.1109/JSAC.2014.141105>
20. Win, M.Z., Scholtz, R.A.: Ultra-wide bandwidth time-hopping spread-spectrum impulse radio for wireless multiple-access communications. *IEEE Trans. Commun.* **48**(4), 679–689 (2000). <https://doi.org/10.1109/26.843135>
21. Hu, B., Beaulieu, N. C.: On characterizing multiple access interference in TH-UWB systems with impulsive noise models. In: 2008 IEEE Radio and Wireless Symposium, pp. 879–882, January 2008. <https://doi.org/10.1109/RWS.2008.4463633>

22. Tan, F., Song, X., Leung, C., Cheng, J.: Collaborative spectrum sensing in a cognitive radio system with laplacian noise. *IEEE Commun. Lett.* **16**(10), 1691–1694 (2012). <https://doi.org/10.1109/LCOMM.2012.080312.120517>
23. Xiaomei Z., Champagne, B., Wei-Ping Z.: Cooperative spectrum sensing based on the RAO test in non-Gaussian noise environments. In: 2013 International Conference on Wireless Communications and Signal Processing, pp. 1–6 (2013). <https://doi.org/10.1109/WCSP.2013.6677074>
24. Wu, J., Wang, C., Yu, Y., Song, T., Hu, J.: Performance optimisation of cooperative spectrum sensing in mobile cognitive radio networks. *IET Commun.* **14**, 1028–1036 (2020). <https://doi.org/10.1049/iet-com.2019.1083>
25. Düzenli, T., Akay, O.: A new spectrum sensing strategy for dynamic primary users in cognitive radio. *IEEE Commun. Lett.* **20**(4), 752–755 (2016). <https://doi.org/10.1109/LCOMM.2016.2527640>
26. Ye, Y., Li, Y., Lu, G., Zhou, F., Zhang, H.: Performance of spectrum sensing based on absolute value cumulation in Laplacian noise. In: 2017 IEEE 86th Vehicular Technology Conference (VTC-Fall), 1–5 September 2017. <https://doi.org/10.1109/VTCFall.2017.8287978>
27. Ye, Y., Li, Y., Lu, G., Zhou, F.: Improved energy detection with Laplacian noise in cognitive radio. *IEEE Syst. J.* **13**(1), 18–29 (2019). <https://doi.org/10.1109/JSYST.2017.2759222>
28. Sinha, K., Trivedi, Y.N.: Spectrum sensing based on dynamic primary user with additive Laplacian noise in cognitive radio. In: Caso, G., De Nardis, L., Gavrilovska, L. (eds.) *CrownCom 2020. LNICSSITE*, vol. 374, pp. 16–28. Springer, Cham (2021). https://doi.org/10.1007/978-3-030-73423-7_2
29. Geddes, K.O., Glasser, M.L., Moore, R.A., et al.: Evaluation of classes of definite integrals involving elementary functions via differentiation of special functions. *Algebra Eng. Commun. Comput.* **1**(2), 149–165 (1990)